Diurnal Pattern of Sun-Induced Chlorophyll Fluorescence as Reliable Indicators of Crop Water Stress

Zhigang Liu, Xue He, Peiqi Yang, Hao Jiang, Shan Xu, Huarong Zhao, Sanxue Ren, and Mi Chen

***Abstract*— Sun-induced chlorophyll fluorescence (SIF) is a promising remote sensing signal for early stress detection due to its close link with photosynthesis. Canopy SIF signals are controlled by leaf physiology, canopy structure, radiation intensity, and sun-observer geometry. Variations in SIF observations are affected by variations in these controlling factors besides water stress. Mitigating the interference of nondrought factors on the variations in canopy SIF to accurately evaluate drought degree is still challenging. In this study, we explore the response of apparent SIF yield (SIF_y) to progressive drought in maize. With experimental evidence, we show that the difference between noon and morning SIF_y was a better indicator of drought than monotemporal SIF_y measurements. We proposed the noon-to-morning ratio (NMR) to characterize diurnal dynamics and assess the severity of drought. The results show that midday measurements of SIF_y were the most affected by water stress, and morning measurements were the least. The NMR of SIF_y successfully revealed water stress by tracking the timing of the transition from light-limited to water-limited conditions of SIF within a day. Hence, the NMRs of SIF_y were considerably more sensitive to drought than their monotemporal values and traditional vegetation indices (VIs), especially during the early phase of drought. This demonstrates that the use of multitemporal or diurnal SIF measurements is more reliable than monotemporal observations for stress detection.**

***Index Terms*— Diurnal dynamics, noon-to-morning ratio (NMR), Sun-induced chlorophyll fluorescence (SIF), water stress.**

Manuscript received 5 February 2023; revised 13 June 2023 and 24 July 2023; accepted 26 July 2023. Date of publication 31 July 2023; date of current version 14 August 2023. This work was supported by the Natural Science Foundation of China under Grant 42071402. *(Corresponding author: Zhigang Liu.)*

Zhigang Liu and Hao Jiang are with the State Key Laboratory of Remote Sensing Science, Faculty of Geographical Science, Beijing Normal University, Beijing 100875, China (e-mail: zhigangliu@bnu.edu.cn; 202121051189@mail.bnu.edu.cn).

Xue He is with the State Key Laboratory of Remote Sensing Science, Faculty of Geographical Science, Beijing Normal University, Beijing 100875, China, and also with the National Geomatics Center of China, Beijing 100830, China (e-mail: xuehe@mail.bnu.edu.cn).

Peiqi Yang is with the Key Laboratory of Virtual Geographic Environment, Ministry of Education, and the Jiangsu Center for Collaborative Innovation in Geographical Information Resource Development and Application, Nanjing Normal University, Nanjing 210023, China (e-mail: p.yang@njnu.edu.cn).

Shan Xu is with the Plant Phenomics Research Centre, Academy for Advanced Interdisciplinary Studies, Nanjing Agricultural University, Nanjing 210095, China (e-mail: xushan@njau.edu.cn).

Huarong Zhao and Sanxue Ren are with the Chinese Academy of Meteorological Sciences, Beijing 100081, China, and also with the Hebei Gucheng Agricultural Meteorology National Observation and Research Station, Baoding 072656, China (e-mail: zhr680317@163.com; 656892rzr@163.com).

Mi Chen is with the College of Resource Environment and Tourism, Capital Normal University, Beijing 100048, China (e-mail: mi.chen@cnu.edu.cn).

Data used is available at https://doi.org/10.6084/m9.figshare.14504919.v2.

Digital Object Identifier 10.1109/LGRS.2023.3300149

I. Introduction

REMOTE sensing has played an increasingly important role in drought studies over the last few decades due to its capability for vegetation monitoring over a large area with a high temporal resolution [1]. Various vegetation indices (VIs) based on canopy reflectance features, such as the normalized difference vegetation index (NDVI) [2], [3] and the enhanced vegetation index (EVI) [4], have been successfully applied in drought monitoring [5]. These greenness-based VIs reveal the loss of leaf, chlorophyll pigment reductions, or leaf curls due to water stress, but they are not sensitive to rapid changes in photosynthetic functions, which can appear at the early phase of stress [6].

Sun-induced chlorophyll fluorescence (SIF), as an effective probe of photosynthesis [7], [8], has been explored as a potential early indicator of plant stress at different spatial scales [9], [10]. To assess water stress with SIF, it is necessary to exclude the confounding factors of SIF, such as the intensity of incoming radiation, canopy structure, and sun-observer geometry. Apparent SIF yield (SIF_y) at top of the canopy (TOC), i.e., the normalization of SIF by incident photosynthetically active radiation (PAR), is commonly used to monitor drought stress as the effect of incoming radiation fluctuations is eliminated [11]. However, the effects of crop growth are not excluded in both SIF and SIF_y for stress detection. On the one hand, water stress can lead to changes in canopy structure and leaf biochemistry, which are detectable from SIF_y or SIF. On the other hand, crop growth certainly also changes the SIF or SIF_y values. As a result, the effects of water stress on SIF and SIF_y cannot be separated from the effects of crop growth. For example, an increase in the leaf area due to crop growth can lead to unchanged or even increased SIF_y or SIF values, which contradicts our knowledge obtained at the photosystem scale.

Several advanced methods have been proposed for the more accurate use of chlorophyll fluorescence to detect drought at both the leaf and canopy scales. At the leaf scale, Flexas et al. [12] proposed normalizing instantaneous chlorophyll fluorescence (F_s) with the dark-adapted intrinsic fluorescence (F_o) to consider the difference between plants due to their different leaf structures, chlorophyll concentrations, and so on. F_o was further applied to correct the ratio of SIF and absorbed PAR and improved the sensitivity of SIF to drought [13]. However, F_o is difficult to obtain for a canopy with passive remote sensing approaches. At the canopy scale, the values of healthy vegetation are employed as a reference for comparison with the values of stressed vegetation. The multiyear averaged SIF or SIF_y values at the same location observed during the periods in the absence of drought are used as a reference value. The departure from the multiyear mean serves as a measure of the level of water stress [3], [14], [15]. Alternatively, the reference value can be obtained from healthy vegetation from the same image [16], [17], [18]. However, the experience of drought (i.e., historic stress) may lead to vegetation growth suppression such that the SIF of vegetation may remain lower than that of normal vegetation even after the relief of water stress. Thus, the departure from the reference is insufficient to determine whether the drought event is impacting the vegetation, even though a lower SIF value is observed. In addition, this method is limited by the availability of healthy vegetation for comparison. Therefore, developing a spatially and temporally applicable drought index based on canopy SIF and SIF_y is still a key problem to be solved.

In this study, a field experiment was conducted, and the diurnal variations in the canopy SIF and SIF_y values of maize with the development of water stress were investigated. We aim to answer the following questions.

1) What are the typical diurnal patterns of canopy SIF and SIF_y under different degrees of water stress?
2) Are the diurnal dynamic characteristics of SIF or SIF_y better indicators of water stress than monotemporal measurements?
3) How can the current water stress be reliably detected with multitemporal remote sensing observations?

II. Materials and Methods

A. Experimental Setup

All analyses were performed in an 8 m^2 (2 × 4 m) experimental plot. The plot is located at the Agricultural Meteorology National Observation and Research Station in Baoding, Heibei, China (39.145°N, 115.738°E). This plot was built with concrete walls and floors to avoid the exchange of soil moisture and nutrients. Over the plot, a movable rain shelter was installed to protect the crop from rainfall such that the soil moisture in the plot can be managed manually.

At the study site, maize (*Zea mays* L.) was planted in a semicontrolled environment. The crop was sown on the 172nd day of the year (DOY) in 2019. Before sowing, the plot was managed according to the common practices and was irrigated to meet the requirements of the early stage of maize growth. During the experiment, the soil moisture of the plot was regulated and controlled by artificial irrigation. After sowing, the plot was irrigated for another two times, at 18:00 local solar time on DOY 216 and 233, when the maize was at the tasseling and silking stage, respectively. Because external rainfall and horizontal exchange of soil moisture were excluded, the soil water content gradually decreased due to evapotranspiration between each of the two irrigations, namely, DOY 172–216 and DOY 216–233. The maize crop gradually developed from a well-watered state on DOY 216 to a water-stressed state on DOY 233, followed by rehydration in the evening on DOY 233.

B. Field Measurements

We collected field measurements after the second irrigation on DOY 216 when the crop was at the vegetative stage, until DOY 266 when the crop was senescent. However, we only selected the data collected on sunny and clear-sky days, namely, on DOY 218, 220, 225, 226, 227, 228, 229, 233, and 236. This period (from DOY 216 to 236) covered the progressive drought from DOY 216 to 233, and the process of recovery after rehydration on DOY 233. Canopy reflectance, canopy SIF, effective canopy leaf area index (LAI_e), and relative soil moisture (RSM) were measured in the experiment.

Continuous canopy reflectance and SIF measurements were collected using the AutoSIF-2–8 (Bergsun Inc., Beijing, China) field spectroscopy system from 08:00 to 17:00 (local solar time) with a time sampling interval of 4–7 min. The system consists of two spectrometers, namely, a QE65Pro spectrometer (Ocean Optics Inc., Dunedin, FL, USA) and an HR2000 spectrometer (Ocean Optics Inc., Dunedin, FL, USA), designed for measuring canopy SIF and reflectance, respectively. The QE65Pro spectrometer collects spectra from 640 to 800 nm with a spectral resolution of ∼0.5 nm full-width at half-maximum (FWHM) and a spectral sampling interval (SSI) of ∼0.2 nm. The HR2000 spectrometer, on the other hand, measures reflectance from 400 to 800 nm with a spectral resolution of ∼1 nm FWHM and an SSI of ∼0.3 nm.

LAI_e was measured by an AccuPAR LP-80 (Decagon Devices, Inc., Pullman, WA, USA) at 8:00 (local solar time) on DOY 218, 225, 226, 228, 233, and 236. Five LAI_e measurements of the maize canopy were randomly sampled. RSM was measured before and after each irrigation. Soil samples were collected at depths of 5, 10, 20, 30, 40, and 50 cm. The RSM values were calculated using the ratio of the gravimetric soil moisture and the moisture holding capacity of the soil, which is described in detail in Zhao et al. [19].

SIF values in two oxygen absorption bands (O_2-A and O_2-B) positioned at 760 nm (SIF_A) and 687 nm (SIF_B) were derived from incident irradiance and upwelling radiance spectra collected with the QE65Pro spectrometer. SIF_A and SIF_B were computed with the spectral fitting method (SFM) [20], assuming a quadratic variation in the reflectance and fluorescence of the absorption band regions. The spectral intervals used for SIF_A and SIF_B estimation were set to 755.63–765.48 nm and 686.30–691.18 nm, respectively. Since the intensity of PAR could be different for individual measurements, the canopy SIF_y was estimated by normalizing the observed SIF for PAR: $SIF_y = SIF/PAR$.

For comparison with the SIF measurements, two widely used VIs, NDVI [21] and EVI [4], were derived from

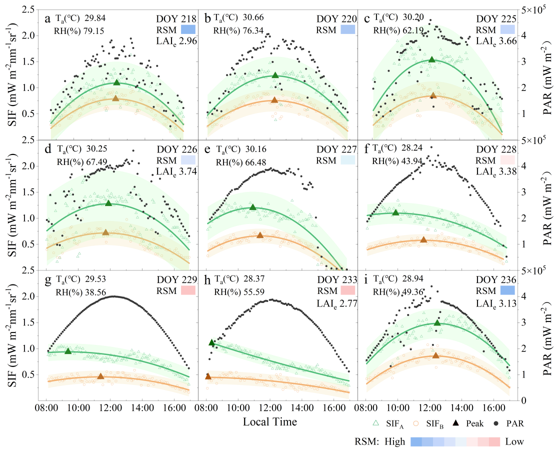

Fig. 1. Observations of incoming PAR (black), SIF$_A$ (green), and SIF$_B$ (brown) from DOY 218 to 236 (a-i) during the evolution of water stress and after rehydration. The solid lines are second-degree polynomial fitting curves for the field measurements with their peaks indicated by the triangles. Shaded areas indicate the 95% predictive interval. The variations in soil moisture are characterized by the RSM. Canopy effective LAI (LAI$_e$) values were measured at 8:00 (local solar time). T_a and RH values are the averaged (from 8:00 to 17:00) air temperature and air relative humidity respectively.

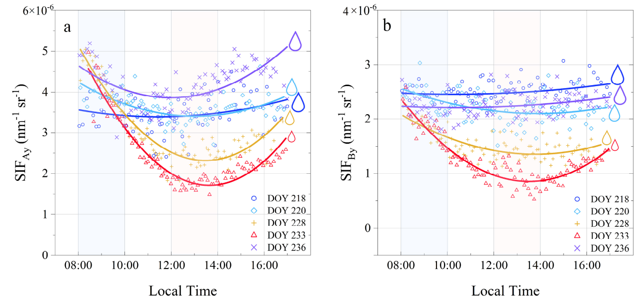

Fig. 2. Observations of SIF$_{Ay}$ (a) and SIF$_{By}$ (b) on DOY 218, 220, 228, 233, and 236 during the progression of drought and after rehydration. The solid lines are second-degree polynomial fitting curves for the field measurements. Variations in the soil moisture are indicated by the size of the water drop shape beside the curve of each day.

reflectance of the QE65Pro spectrometer and from that of the HR2000 spectrometer, respectively.

C. Characterization of the Diurnal Patterns

Monotemporal measurements of SIF are affected by both drought and nondrought factors (e.g., incident radiation and crop growth) and thus are limited in detecting water stress of crops. We propose to use the diurnal continuous measurements of SIF$_y$ to explore the response of crops to water stress. In addition to the diurnal curves of SIF$_y$, we propose taking the ratios of SIF$_y$ measured in the noon and in the morning to characterize the diurnal pattern

$$\mathrm{NMR}_{\mathrm{SIF\_y}} = \frac{\overline{\mathrm{SIFy}}_{12:00-14:00}}{\overline{\mathrm{SIFy}}_{08:00-10:00}} \tag{1}$$

where $\overline{\mathrm{SIFy}}_{08:00-10:00}$ and $\overline{\mathrm{SIFy}}_{12:00-14:00}$ denote the mean SIF$_y$ at noon (from 12:00 to 14:00) and in the morning (from 08:00 to 10:00), respectively. The idea of the noon-to-morning ratio (NMR) of SIF$_y$ is to mitigate the effect of nondrought factors and to isolate the water-stress effect on SIF observations. As a comparison, the NMR of the VIs (EVI and NDVI) was computed as well

$$\mathrm{NMR}_{\mathrm{VI}} = \frac{\overline{\mathrm{VI}}_{12:00-14:00}}{\overline{\mathrm{VI}}_{08:00-10:00}}. \tag{2}$$

III. Results

A. SIF and SIF$_y$ Under Different Water Stress Levels

Fig. 1 shows the observations of SIF and incident PAR, and RSM and LAI$_e$ on nine sunny days between DOY 216 and 236. The daily averaged SIF showed substantial variation due to crop growth and water stress. The crop suffered from water stress progressively from DOY 218 to 233 and was rehydrated on the evening of DOY 233. During the period from DOY 218 to 233, the soil moisture content was constantly decreasing. Unlike the soil moisture, SIF$_A$ and SIF$_B$ did not decrease accordingly. Instead, they gradually increased at first from DOY 218 to 226 [Fig. 1(a)–(d)] and then decreased afterward [Fig. 1(e)–(h)]. The initial increase in SIF complied with the growth of the crop indicated by the increase in LAI$_e$, while the decrease in SIF after DOY 226 complied with the severity of water stress indicated by the decrease in RSM. The increase in TOC SIF complies with the increase in LAI$_e$, which changed from 2.96 m^2/m^2 on DOY 218 to 3.66 m^2/m^2 on DOY 225 due to maize growth. In comparison, both LAI$_e$ and the daily averaged SIF declined after DOY 226 due to limited water supply, but they clearly recovered after the rehydration on the evening of DOY 233. The daily SIF on DOY 233 recovered to the similar level as on DOY 220 [Fig. 1(g)].

Fig. 2 presents TOC SIF$_y$, which attempts to minimize the effects of incoming radiation on observed SIF. For the sake of simplicity, SIF$_y$ on five days were plotted. Compared with SIF, the intensity of SIF$_y$ was less sensitive to the intensity of incoming light. The observed TOC SIF values fluctuated widely under unstable illumination [e.g., Fig. 1(d)], making it difficult to assess drought intensity based on SIF values alone under natural conditions. Normalized by the PAR values, the diurnal trends of SIF$_y$ were more stable than those of SIF. It is clear that SIF$_y$ was much smaller when the soil moisture was lower. When the drought stresses were relatively severe (from DOY 226 to 233), the values of SIF and SIF$_y$ at midday obviously decreased with the aggravation of drought. In contrast, in the early morning, the magnitude of SIF$_{Ay}$ tended to increase with increasing LAI$_e$ [Fig. 2(a)], and there was no correlation with water stress intensity. The morning values of SIF$_{By}$ did not increase with increasing LAI$_e$ [Fig. 2(b)].

However, due to the influence of growth, even the values of SIF and SIF$_y$ at midday were not a reliable drought indicator. During the period from DOY 218 to 225, although the soil moisture content was decreasing, SIF$_A$ and SIF$_B$ gradually increased in magnitude [Fig. 1(a)–(c)]. For SIF$_{Ay}$, the midday values on DOY 236 after rehydration were obviously larger than those on DOY 218 [Fig. 2(a)], which may be due to an increase in LAI rather than the difference in water stress.

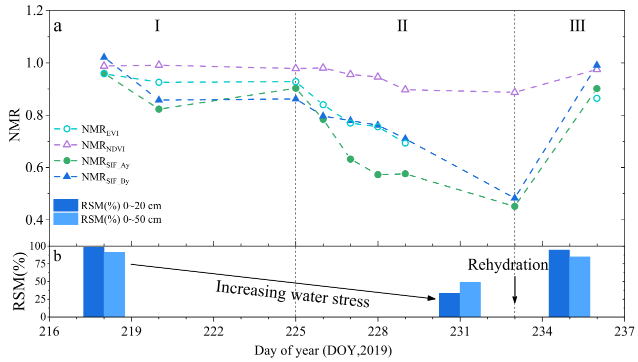

Fig. 3. Variation in the NMR values of NDVI (purple), EVI (cyan), SIF_{Ay} (green), and SIF_{By} (blue) in the process of increasing water stress and after rehydration. (a) Histogram in (b) shows the decrease of RSM.

B. Differences in Diurnal Patterns of SIF and SIF_y

Figs. 1 and 2 also show that the diurnal patterns of SIF and SIF_y during the drought had a prominent diurnal dynamic feature. As expected, in the absence of water stress, SIF_A and SIF_B changed correspondingly, with the incident PAR increasing from morning to midday and then declining afterward. On sunny days, the maximal values of SIF within a day appeared around solar noon (i.e., maximal PAR), and the diurnal observations of both the red and far-red SIF were symmetric to solar noon [Fig. 1(a) and (b)]. In stark contrast, the diurnal patterns of TOC SIF for the stressed crops did not change proportionally in response to the incoming radiation. With the increase in drought, the occurrence of diurnal peaks of both SIF_A and SIF_B shifted gradually from midday to early morning [Fig. 1(c)–(h)]. As a result, the diurnal patterns of SIF were not symmetric around solar noon when the crop was stressed. After rehydration, the diurnal measurements of SIF_A and SIF_B quickly recovered, as indicated by the appearance of this symmetrical pattern.

The diurnal patterns of SIF_y of the drought-stressed canopy were distinctly different from those of the well-water canopy (Fig. 2). In the absence of drought, the diurnal profiles of both SIF_{Ay} and SIF_{By} were symmetrical, with their minimums appearing in the early afternoon. However, the variability was relatively small over the course of a day. During drought stress, SIF_{Ay} and SIF_{By} declined in the morning to reach their minima in the early afternoon at approximately 13:00, recovering in the afternoon to a level lower than that in the morning. After rehydration at night on DOY 233, the diurnal profile of SIF_{Ay} on DOY 236 became symmetric again.

C. Dynamics of the NMRs

Fig. 3 shows the variation curves of the NMRs of SIF_{Ay}, SIF_{By}, NDVI, and EVI throughout the whole drought and rehydration period. According to the differences in the variation degree of NMR, we distinguished three phases in the experiment. The first phase (DOY 218–225) was the mild water stress phase. No obvious changes in NMR_{NDVI} were observed, and NMR_{EVI} decreased slightly. However, NMR_{SIF_Ay} and NMR_{SIF_By} declined more notably, roughly changing from 1 to 0.8. During a second phase (DOY 225–233), NMR_{NDVI}, NMR_{EVI}, NMR_{SIF_Ay}, and NMR_{SIF_By} showed a continuous and larger decrease simultaneously. NMR_{SIF_Ay} had the steepest decline curve, followed by NMR_{SIF_By} and NMR_{EVI}, and NMR_{NDVI} had the smoothest decline curve. When the drought stress was at its most severe on DOY 233, the values of NMR_{SIF_Ay} and NMR_{SIF_By} were approximately 0.5. The NMR_{EVI} on DOY 233 was not available due to failure of the instrument in the morning. Rehydration was implemented on the night of DOY 233. The period lasting from this evening to DOY 236 was the third phase, in which the drought was relieved. On DOY 236, the NMR values of all parameters recovered to the values they were at the beginning of the first phase.

IV. Discussion

A. Water Stress and Radiation on Canopy SIF

Canopy SIF and SIF_y of the investigated crop were affected by available radiation, soil moisture, and canopy structure [22]. During the experiment, the investigated crops were affected by water deficit, causing a case of resource imbalance. When radiation is sufficient (e.g., in the midday), water is limited, and plants cannot redirect their potential to utilize other resources and consequently tend to decrease investment in the light harvest [23]. In contrast, when SIF is limited by the available radiation (e.g., in the early morning), air temperature is low, water is sufficient for plants' evapotranspiration, and plants tend to increase investment in light harvest (Fig. 1). We observed a transition of light-to-water-limited canopy SIF from the early morning to midday. Moreover, we observed a quicker transition with the development of water stress. When the crop became more stressed, the water-limited conditions of canopy SIF occurred at lower radiation levels. This was indicated by the shifting of the maximal SIF values from midday toward morning (Fig. 1). Our findings are overall consistent with the current understanding of the response of fluorescence to light: water stress causes the transition from a light-limited to a light-saturated state at a lower light intensity and results in a decrease in the fluorescence yield [24].

B. Rational of NMRs

When there is sufficient water for the crop, the available radiation (i.e., PAR) dominates the intensity of SIF. Hence, to evaluate the severity of water stress, SIF measurements ought to be taken during water-limited conditions. The midday measurements are, therefore, preferred over the morning measurements. As shown in Figs. 1 and 2, SIF and SIF_y in the middays showed the largest variation in the midday. However, SIF measurements were also largely affected by crop growth. Changes in LAI_e had a significant effect on the variation in SIF. During the period from DOY 218 to 225, although the soil moisture content was constantly decreasing, SIF_A and SIF_B in middays gradually increased in magnitude [Fig. 1(a)–(c)]. As a result, the variation in SIF or SIF_y might not reveal the severity of water stress. This suggests that due to the disturbance of crop growth, it is difficult to assess drought intensity by the magnitude of SIF and SIF_y with observations at a single moment, and diurnal dynamics are needed.

Based on the diurnal pattern of SIF and SIF_y under water stress, we propose the NMR to evaluate the degree of water stress. We consider that SIF observations in the morning and midday are both affected by nondrought factors, such as crop growth, but midday's measurements are most affected by the drought and morning measurements are least affected. By taking the ratio between the values in the midday and morning, the nondrought factors can be partially corrected, while the drought effects on SIF are enhanced. Compared with NDVI and EVI, NMR of SIF and SIF_y is less pronounced to the saturation problem [25]. Moreover, SIF and SIF_y also contain information on physiological variation such that they were more sensitive to water stress than NDVI and EVI. The limitation of NMR is that it requires clear weather in the morning and noon periods.

V. Conclusion

Our study confirms that SIF is a novel stress indicator related to the physiological response of plants and complements reflectance information that mainly responds to biochemical and structural canopy responses. To eliminate inferences by the nondrought factors, the NMR was proposed to measure the degree of drought in a given day. The sensitivity of SIF_y NMR to drought was higher than that of the NDVI and EVI, especially during the mild drought phase. We recommend the use of multitemporal or diurnal measurements of SIF and SIF_y over monotemporal measurements for drought detection. The findings of this study support the design of operational approaches for crop stress detection from space.

References

[1] W. Jiao, L. Wang, and M. F. McCabe, "Multi-sensor remote sensing for drought characterization: Current status, opportunities and a roadmap for the future," *Remote Sens. Environ.*, vol. 256, Apr. 2021, Art. no. 112313, doi: 10.1016/j.rse.2021.112313.

[2] Y. Bayarjargal, A. Karnieli, M. Bayasgalan, S. Khudulmur, C. Gandush, and C. Tucker, "A comparative study of NOAA–AVHRR derived drought indices using change vector analysis," *Remote Sens. Environ.*, vol. 105, no. 1, pp. 9–22, Nov. 2006, doi: 10.1016/j.rse.2006.06.003.

[3] S. Wang, C. Huang, L. Zhang, Y. Lin, Y. Cen, and T. Wu, "Monitoring and assessing the 2012 drought in the great plains: Analyzing satellite-retrieved solar-induced chlorophyll fluorescence, drought indices, and gross primary production," *Remote Sens.*, vol. 8, no. 2, p. 61, Jan. 2016.

[4] A. R. Huete, K. Didan, T. Miura, E. P. Rodriguez, X. Gao, and L. G. Ferreira, "Overview of the radiometric and biophysical performance of the MODIS vegetation indices," *Remote Sens. Environ.*, vol. 83, nos. 1–2, pp. 195–213, 2002, doi: 10.1016/S0034-4257(02)00096-2.

[5] H. West, N. Quinn, and M. Horswell, "Remote sensing for drought monitoring & impact assessment: Progress, past challenges and future opportunities," *Remote Sens. Environ.*, vol. 232, Oct. 2019, Art. no. 111291, doi: 10.1016/j.rse.2019.111291.

[6] O. Ghannoum, "C_4 photosynthesis and water stress," *Ann. Botany*, vol. 103, no. 4, pp. 635–644, May 2008, doi: 10.1093/aob/mcn093.

[7] N. R. Baker, "Chlorophyll fluorescence: A probe of photosynthesis in vivo," *Annu. Rev. Plant Biol.*, vol. 59, no. 1, pp. 89–113, Jun. 2008, doi: 10.1146/annurev.arplant.59.032607.092759.

[8] G. H. Mohammed et al., "Remote sensing of solar-induced chlorophyll fluorescence (SIF) in vegetation: 50 years of progress," *Remote Sens. Environ.*, vol. 231, Sep. 2019, Art. no. 111177, doi: 10.1016/j.rse.2019.04.030.

[9] A. A. Z. Malenovský, J. Olejníčková, A. Gallé, U. Rascher, and G. Mohammed, "Meta-analysis assessing potential of steady-state chlorophyll fluorescence for remote sensing detection of plant water, temperature and nitrogen stress," *Remote Sens. Environ.*, vol. 168, pp. 420–436, Oct. 2015, doi: 10.1016/j.rse.2015.07.022.

[10] F. Jonard et al., "Value of sun-induced chlorophyll fluorescence for quantifying hydrological states and fluxes: Current status and challenges," *Agricult. Forest Meteorol.*, vol. 291, Sep. 2020, Art. no. 108088, doi: 10.1016/j.agrformet.2020.108088.

[11] P. Yang, C. van der Tol, P. K. E. Campbell, and E. M. Middleton, "Fluorescence correction vegetation index (FCVI): A physically based reflectance index to separate physiological and non-physiological information in far-red sun-induced chlorophyll fluorescence," *Remote Sens. Environ.*, vol. 240, Apr. 2020, Art. no. 111676, doi: 10.1016/j.rse.2020.111676.

[12] J. Flexas et al., "Steady-state chlorophyll fluorescence (Fs) measurements as a tool to follow variations of net CO_2 assimilation and stomatal conductance during water-stress in C_3 plants," *Physiologia Plantarum*, vol. 114, no. 2, pp. 231–240, Feb. 2002, doi: 10.1034/j.1399-3054.2002.1140209.x.

[13] L. T. Helm, H. Shi, M. T. Lerdau, and X. Yang, "Solar-induced chlorophyll fluorescence and short-term photosynthetic response to drought," *Ecol. Appl.*, vol. 30, no. 5, Jul. 2020, Art. no. e02101, doi: 10.1002/eap.2101.

[14] W. Jiao, Q. Chang, and L. Wang, "The sensitivity of satellite solar-induced chlorophyll fluorescence to meteorological drought," *Earth's Future*, vol. 7, no. 5, pp. 558–573, May 2019, doi: 10.1029/2018EF001087.

[15] Y. Sun et al., "Drought onset mechanisms revealed by satellite solar-induced chlorophyll fluorescence: Insights from two contrasting extreme events," *J. Geophys. Res., Biogeosci.*, vol. 120, no. 11, pp. 2427–2440, Nov. 2015, doi: 10.1002/2015JG003150.

[16] M. Rossini et al., "Discriminating irrigated and rainfed maize with diurnal fluorescence and canopy temperature airborne maps," *ISPRS Int. J. Geo-Inf.*, vol. 4, no. 2, pp. 626–646, Apr. 2015.

[17] S. Wieneke et al., "Airborne based spectroscopy of red and far-red sun-induced chlorophyll fluorescence: Implications for improved estimates of gross primary productivity," *Remote Sens. Environ.*, vol. 184, pp. 654–667, Oct. 2016, doi: 10.1016/j.rse.2016.07.025.

[18] P. J. Zarco-Tejada, M. V. González-Dugo, and E. Fereres, "Seasonal stability of chlorophyll fluorescence quantified from airborne hyperspectral imagery as an indicator of net photosynthesis in the context of precision agriculture," *Remote Sens. Environ.*, vol. 179, pp. 89–103, Jun. 2016, doi: 10.1016/j.rse.2016.03.024.

[19] L. Zhao, Z. Liu, S. Xu, X. He, Z. Ni, H. Zhao, and S. Ren, "Retrieving the diurnal FPAR of a maize canopy from the jointing stage to the tasseling stage with vegetation indices under different water stresses and light conditions," *Sensors*, vol. 18, p. 3965, 2018.

[20] M. Meroni, L. Busetto, R. Colombo, L. Guanter, J. Moreno, and W. Verhoef, "Performance of spectral fitting methods for vegetation fluorescence quantification," *Remote Sens. Environ.*, vol. 114, no. 2, pp. 363–374, Feb. 2010, doi: 10.1016/j.rse.2009.09.010.

[21] J. W. Rouse, R. H. Haas, D. W. Deering, and J. A. Schell, "Monitoring the vernal advancement and retrogradation (green wave effect) of natural vegetation," Texas A&M Univ., College Station, TX, USA, Progress Rep. RSC 1978-2, 1974.

[22] P. Yang and C. van der Tol, "Linking canopy scattering of far-red sun-induced chlorophyll fluorescence with reflectance," *Remote Sens. Environ.*, vol. 209, pp. 456–467, May 2018, doi: 10.1016/j.rse.2018.02.029.

[23] S. P. Long, S. Humphries, and P. G. Falkowski, "Photoinhibition of photosynthesis in nature," *Annu. Rev. Plant Biol.*, vol. 45, no. 1, pp. 633–662, 1994.

[24] C. Tol, J. A. Berry, P. K. E. Campbell, and U. Rascher, "Models of fluorescence and photosynthesis for interpreting measurements of solar-induced chlorophyll fluorescence," *J. Geophys. Res., Biogeosci.*, vol. 119, no. 12, pp. 2312–2327, Dec. 2014, doi: 10.1002/2014JG002713.

[25] X. Yang et al., "Solar-induced chlorophyll fluorescence that correlates with canopy photosynthesis on diurnal and seasonal scales in a temperate deciduous forest," *Geophys. Res. Lett.*, vol. 42, no. 8, pp. 2977–2987, Apr. 2015, doi: 10.1002/2015GL063201.